Automotive and Engine Technology (2023) 8:1–16
https://doi.org/10.1007/s41104-022-00123-7

ORIGINAL PAPER

# Concept evaluation of a P2 MHEV SUV: application for possible EU7 boundaries

Hannes Wancura[1] · Gabriel Kühberger[2] · Eberhard Schutting[2]

Received: 25 February 2022 / Accepted: 10 November 2022 / Published online: 2 January 2023


## Abstract
In this work, the experimental results that appeared in the recent published article "Current experimental developments in 48 V-based CI-driven SUVs in response to expected future EU7 legislation" are used to create a proper system simulation model with the simulation platform AVL CRUISE$^{TM}$ M. This simulation model is then used to perform a system validation in order to evaluate the configuration with a straight-four compression ignition (CI) engine and the selected exhaust aftertreatment system (EAS). The mild hybrid electric vehicle (MHEV) has an 48 V P2 architecture and an 8-gear dual-clutch transmission (DCT) as a powertrain configuration. In addition to evaluating the 48 V potential, the simulation is performed with a conventional 12 V configuration, but also including an electrically heated catalyst (EHC). As boundary conditions for the simulation, we use the different engine operating mode (EOM) calibrations from the test bed to trigger the dedicated operation modes of the internal combustion engine (ICE). For the exhaust aftertreatment system (EAS), an optimization loop is performed to obtain a layout which will be near a serial production. This includes optimizing the heat losses and reducing the thermal mass of the canning. Beside the plant models, a hybrid control unit (HCU) is used, which includes an exhaust aftertreatment system coordinator (EASC). With these functionalities, the EOMs, electrically heated catalyst (EHC), electric machine (EM) and dosing control unit (DCU) are optimized to obtain the lowest possible nitrogen oxides ($NO_x$) with an carbon dioxide ($CO_2$) reduction potential. The targets for the emission limits are defined on the basis of the available information from the Consortium for ultra-Low Vehicle Emissions (CLOVE) and International Council on Clean Transportation (ICCT) proposals.

**Keywords** Emission legislation · Exhaust aftertreatment · Electrically heated catalyst · Mild hybrid vehicle · 48 V P2 · EU 7

### Abbreviations

| | |
|---|---|
| ASC | Ammonia slip catalyst |
| BEV | Battery electric vehicle |
| BMEP | Brake mean effective pressure |
| BSFC | Brake-specific fuel consumption |
| CC | Close-coupled |
| CF | Conformity factor |
| $CH_4$ | Methane |
| CI | Compression ignition |
| CLOVE | Consortium for ultra-Low Vehicle Emissions |
| CO | Carbon monoxide |
| $CO_2$ | Carbon dioxide |
| CPSI | Cells per square inch |
| DCT | Dual-clutch transmission |
| DCU | Dosing control unit |
| DOC | Diesel oxidation catalyst |
| DoE | Design of experiments |
| EAS | Exhaust aftertreatment system |
| EASC | Exhaust aftertreatment system coordinator |
| ECU | Engine control unit |
| EHC | Electrically heated catalyst |
| EM | Electric machine |
| EO | Engine out |
| EOM | Engine operating mode |
| EU | European Union |

✉ Gabriel Kühberger
gabriel.kuehberger@gmail.com

Hannes Wancura
hannes.wancura@avl.com

Eberhard Schutting
schutting@ivt.tugraz.at

[1] AVL List GmbH, Graz, Austria

[2] Institute of Thermodynamics and Sustainable Propulsion Systems, Graz University of Technology, Graz, Austria

| | |
|---|---|
| EV | Electric vehicle |
| FSN | Filter smoke number |
| FC | Fuel consumption |
| HC | Hydrocarbons |
| HCU | Hybrid control unit |
| HP-EGR | High pressure exhaust gas recirculation |
| HW | Highway |
| ICE | Internal combustion engine |
| ICCT | International Council on Clean Transportation |
| LCV | Light commercial vehicle |
| LNT | Lean $NO_x$ trap |
| LPD | Load point down-shifting |
| LPU | Load point up-shifting |
| MHEV | Mild hybrid electric vehicle |
| NEDC | New European Driving Cycle |
| $NH_3$ | Ammonia |
| NMOG | Non-methane organic gases |
| $NO_x$ | Nitrogen oxides |
| $N_2O$ | Laughing gas |
| OEM | Original equipment manufacturer |
| PC | Passenger car |
| RDE | Real driving emissions |
| SCR | Selective catalytic reduction |
| SDPF | Diesel particulate filter with SCR coating |
| SoC | State of charge |
| SUV | Sport utility vehicle |
| THC | Total hydrocarbons |
| TfL | Transport for London cycle |
| TP | Tailpipe |
| UF | Underfloor |
| VGT | Variable-geometry turbocharger |
| WLTC | Worldwide harmonized Light-duty vehicles Test Cycle |
| w/ | With |
| w/o | Without |

## 1 Introduction

The New European Driving Cycle (NEDC) was enacted in 1991 for comparable exhaust gas and fuel consumption measurement of passenger cars (PCs) in the European Union (EU) [1]. This driving cycle allowed a lot of leeway in its execution and was not very close to reality [6]. The first package and thus the introduction of Real Driving Emissions (RDE) was finally published in 2016, several years after the European Commission had already established a working group in 2011 to develop a test procedure for measuring exhaust gas under real-world operation conditions [10]. The International Council on Clean Transportation (ICCT) presented real emission measurement results of EU 6 vehicles in 2014 and already in September 2015 the emissions scandal began [6]. As a result, diesel technology was marked as "dirty" in general and trust in this technology waned, while many discussions arose over the city ban. Also at this time, other applications appeared which were well below the nitrogen oxides ($NO_x$) emission legislation level limits for EU 6b, but these were disregarded.

As a consequence due to emissions exceedances and to complete this legislation step, every original equipment manufacturer (OEM) was required to sell a propulsion system that is in compliance with the emission legislation also in real driving, whether the vehicle is diesel- or gasoline-fueled. In the EU 6d TEMP and FINAL stages [11], the emission stability and the applied hardware were finally improved significantly. Recent investigations also have shown that the new certification means consistently good news for the diesel technology [19]. Finally, it has still not been possible to increase the diesel share in the European Union (EU) and to return to the market situation that existed before the Dieselgate scandal. The technology package for smaller applications was too cost intensive for the market. Thus, most of the OEMs excluded them from their portfolios and focused on battery electric vehicles (BEVs) and gasoline-fueled PCs.

For EU 7, the diesel engine in its hybrid form is presumably still able to meet the market qualifications. The cost level of these engines will be similar to that of gasoline-fueled powertrains—especially considering zero impact emissions [5]. Latest research indicates, that the proposed EU 7 regulation comply with zero emissions impact requirements in terms of air quality; i.e. vehicles fulfilling EU 7 have an insignificant impact to the air quality in terms of $NO_x$ and particles [20]. For heavier vehicles like the sport utility vehicle (SUV) or the light commercial vehicle (LCV), clean diesel technology has certain benefits and is required, considering a worldwide market [12]. By preparing a proper technology package, therefore, it is possible to gain a carbon dioxide ($CO_2$) advantage with respect to the competitive gasoline internal combustion engine (ICE) at comparable or even improved costs for the customer. This is the reason for the investigations and results presented. Based on test bed measurements of a heavy sport utility vehicle (SUV) a simulation model is set up and various comparisons and conclusions are drawn out of it. The main focus is on low $NO_x$ and laughing gas ($N_2O$) emissions.

## 2 Methodology and simulation model

This work represents a continuation of the experimental work described in the recently published article entitled "Current experimental developments in 48 V-based CI-driven SUVs in response to expected future EU 7 legislation" [3]. In the current study, we use the test bed data to create a complete vehicle model. This model contains the plant models for internal combustion engine (ICE), exhaust aftertreatment system (EAS) and powertrain (12 V as well as 48 V components), including the required software functionalities to apply appropriate control for the plant models. To model the simulation platform, AVL CRUISE™ M and Model.CONNECT™ are used (Fig. 1). Via Model.CONNECT all sub models where connected using a separation of information and physical data. For each submodel a specific modeling approach was used. The aftertreatment is built with 1D catalyst models with the required reactions. The Engine and the airpath is built with throttle and volume elements (0D approach), where the turbocharger is modeled with a specific turbocharger tool and the cylinder is based on the MOBEO approach [24]. If the complexity and the real time capability allows a physical modeling is applied like $NO_x$, Temperature, BMEP, MFB50 and the other calculations are empirical, like the emissions CO, THC and Soot. This enables the implementation of Simulink-based controllers. For a comprehensive description of the underlying modeling approaches, assumptions and boundary conditions, please refer to literature [4, 21–23, 25].

## 2.1 Submodels

This section gives an overview of the characteristics of the engine, the powertrain including the 48 V components and the EAS. For the ICE, the powertrain and the EAS, the same hardware is used as in the former investigations (cf. [3]). For

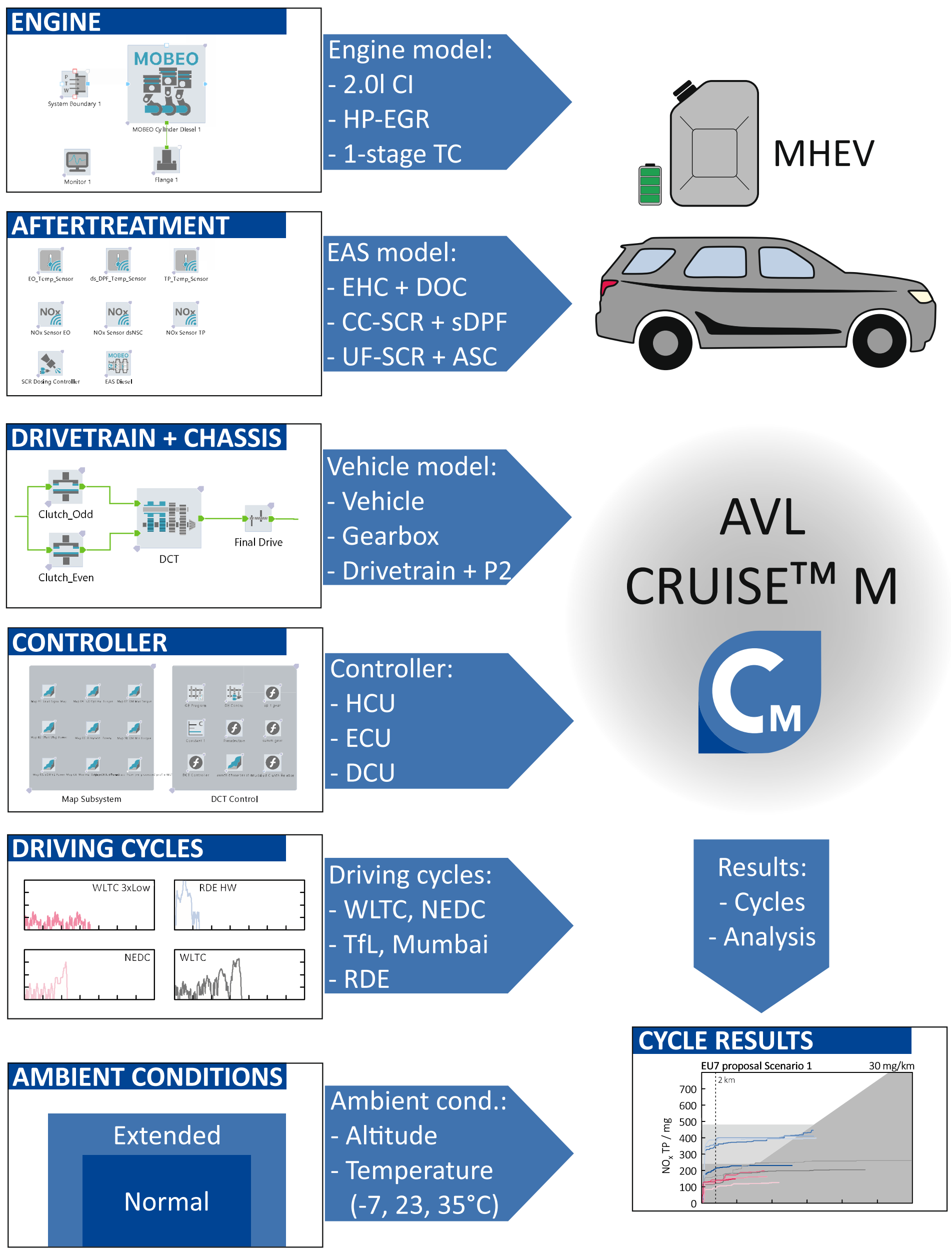


**Fig. 1** AVL CRUISE™ M environment and submodels with main parameters, including inputs and outputs

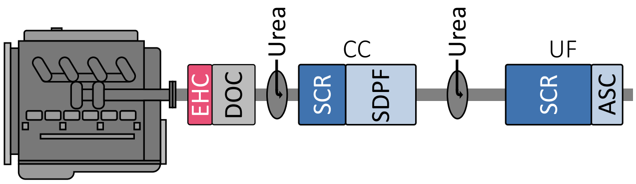


**Fig. 2** Exhaust aftertreatment system

the 48 V components, we use the characteristics from the models, which were previously published in another journal (cf. [8, 26]). The properties of the electric machine (EM) are also obtained from a former publication (cf. [7]). The main properties of ICE, EM and EAS are listed in the Appendix in Tables 1 and 2.

To provide an brief overview, the whole EAS is schematically shown in Fig. 2. It consists of a Diesel Oxidation Catalyst (DOC) including an electrically heated catalyst (EHC) and a selective catalytic reaction (SCR) double dosing unit. The close-coupled (CC) system contains a SCR and diesel particulate filter with SCR coating (SDPF), while the underfloor (UF) system also consists of a SCR and an ammonia slip catalyst (ASC). The total volume of the catalysts is slightly below 12 l.

## 2.2 Controller

In addition to controlling the plant models, it is important to control all the actuators in the simulation environment. For this purpose, the engine control unit (ECU) software is calibrated to operate the ICE in all required engine operating modes EOMs. This includes the:
*Air path*

- High pressure exhaust gas recirculation (HP-EGR) including the cooler bypass
- Variable-geometry turbocharger (VGT)
- Intake throttle valve

*Injection path*

- Quantities, timings and durations of the two pilot injections, the main injection, the early post-injection and the late post-injection
- Injection pressure

*Exhaust aftertreatment system*

Regarding the aftertreatment, a controller for the dual stage SCR system is required that takes into account the CC- and the UF-SCR. The ammonia ($NH_3$) buffer is the main parameter that affects ($NO_x$) conversion efficiency, whereby the ($NH_3$) slip affects the demand values for the control. The heating grid (EHC) is included in the EAS, and this grid includes a functionality that targets the SCR temperature. In addition to the main parameter, the SCR temperature, the maximum DOC and the maximum heater grid temperature are considered. The available heating power is defined by the 48 V board net.

The 48 V components are controlled by the hybrid control unit (HCU) and the exhaust aftertreatment system coordinator (EASC) in the powertrain. Here, the conventional hybrid functionalities [8, 26] and EAS-relevant functionalities, including the EHC controller, are set up. The EASC limits the ICE torque during the heat-up period, enabling the system to reach a mass flow range that is optimal for the EAS. This optimum mass flow is determined via the future state of the EAS, i.e., using a prediction approach via the enthalpy stream. The calculation method and parameters are based on previous investigations (cf. [8]) and transferred via the principle of similarity. Both the heat-up and the keep-warm are triggered by the EASC-functionality. The optimum measure is selected on the basis of the current $NO_x$ (in mg/km) and the $CO_2$ (in g/km) in the tailpipe. To consider the impact of different ambient conditions on the vehicle performance, a board net load is defined, whereby the impact of the air conditioning and/or heating devices is determined. Depending on the battery condition $f(T, aging)$, the electrical consumption may be limited. However, the main priority is the compliance with emissions legislation.

*Mild hybrid electric vehicle (MHEV) operation modes*

In general, a forward model is used, which is rule based. In the following sections, the results of an evaluation of the different possible operation modes of the MHEV support are reported. Therefore, a short explanation of these modes is provided. The activation areas for the modes are also shown schematically in Fig. 3, whereby the permissible ranges are presented in dark gray depending on the usable state of charge (SoC).

- Load point up-shifting (LPU)
- Load point down-shifting (LPD)

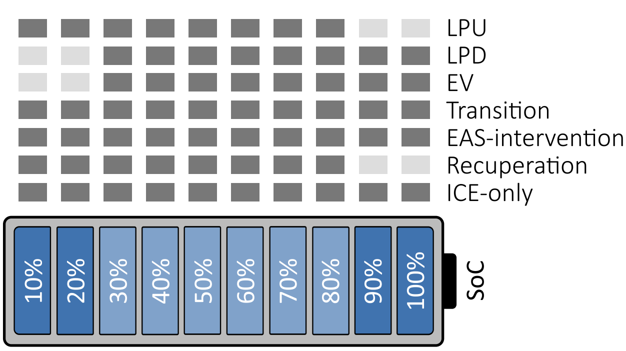


**Fig. 3** Hybrid functionalities and activation areas

- EAS intervention (LPU + LPD)
- Electric vehicle (EV): pure electric driving; ICE off
- Transitions: all transitions between the trigger modes in the HCU
- Recuperation: energy recuperation during active vehicle braking; ICE off or on
- ICE only: pure ICE operation

In the Figure, the usable SoC of the battery is shown from 0% to 100%. In this area, the battery has a normal aging and linear voltage behavior. There is still the possibility to go above and below the SOC level, but then the voltage will decrease/increase rapidly and the aging will accelerate. For the normal operation, the hybrid controller will ensure the light blue shaded range between 20% and 80%. If 0% SOC is reached the system requires an external loading to ensure voltage and aging stability.

## 2.3 Vehicle simulation

The adaptation of the simulation environment includes the engine and the aftertreatment. Therefore, the existing models are adapted to the target applications in order to simulate the system. The baseline for the powertrain configuration and the 48 V components are taken from an existing environment for which all required information (performance and efficiencies, depending on different temperatures and aging conditions) is available. Based on the hardware status from the engine test bed, the canning of the EAS, optimization of the thermal mass and the heat losses that are applied are mainly considered. Regarding the coating technology, all information is adopted from the characterization of the hardware performed on the engine test bench [3]. It is necessary to adapt these components to the target application, and the vehicle validation was repeated to fit the available test bed data.

As already mentioned, a heavy SUV is considered in its hybrid form (MHEV). The driving resistance parameters are given in Table 3. During the test bench and simulation phases, special consideration is given to the expected future EU 7 legislation [2].

## 2.4 Validation of simulation model

To estimate the model's accuracy and capabilities, a comparison is made between the simulation and measurement results gained from the engine test bed. The validation of the model in this section is showing the correlation of the Engine out position, were the Engine model and the Software ECU are in the focus. The alignment of the EAS was done in a separate loop, also the parametrization of the Engine itself. The idea was to keep the validation phase as short as possible. As an first example, the transient correlations under a 25 °C ambient condition are shown in Fig. 4 for a WLTC.

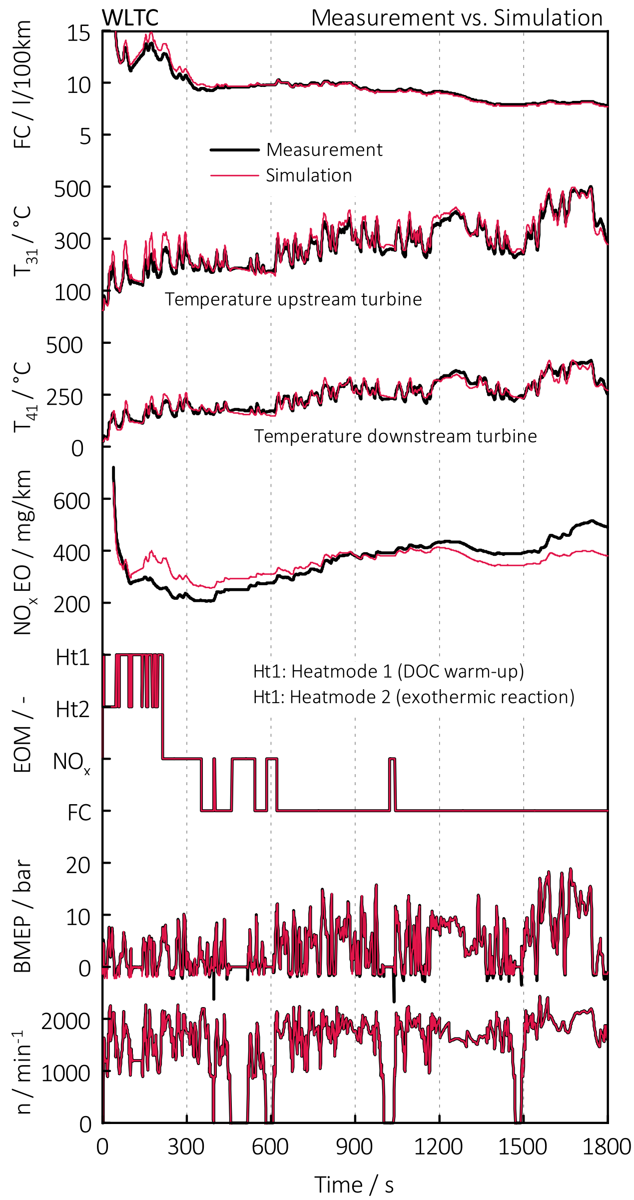


**Fig. 4** Comparison measurement vs. simulation in WLTC

The deviation of the fuel consumption between measurement and simulation is very low. The differences concerning $NO_x$ at engine-out (EO) measurement position in the WLTC are the result out of the best consistency not only in the WLTC but even with other cycles, as will be shown later. In this cycle, a small overestimation exists in the first phase "Low" of the cycle, while an underestimation exists in the last phases "High" and "Extra High". The temperature curves at measurement position $T_{31}$ (upstream of the turbine) also match very closely. Only in the first 300 s a small overestimation in the temperature peaks exists. The traces for the brake mean effective pressure (BMEP), engine speed and the selection of the EOMs are taken from the measured cycle and given in the simulation for the alignment. In total, four EOMs exist. These are "Heatmode 1", "Heatmode 2", "Low $NO_x$" and "Low fuel consumption (FC)". The calibration is taken from the stationary measurements performed on the test bench.

It was possible to adjust the simulation effectively using the comprehensive model and test bed measurement data of six driving cycles in total. The measurement data out of the test bed for the standard heavy SUV was always used for the adjustment of the simulation model. The evaluation of a lighter application in Fig. 16 is purely determined by changing the longitudinal dynamics simulation. A measurement-based adjustment is not possible due to lack of measurement data.

Additionally the alignment for one low-load (Fig. 5) and one high-load driving cycle (Fig. 6) is shown both for 25 °C as well as for −5 °C. Goal of the modeling activity was to set up a proper work environment to extend the limited possibilities from the engine test bed by considering a complete vehicle and a hybrid architecture [3].

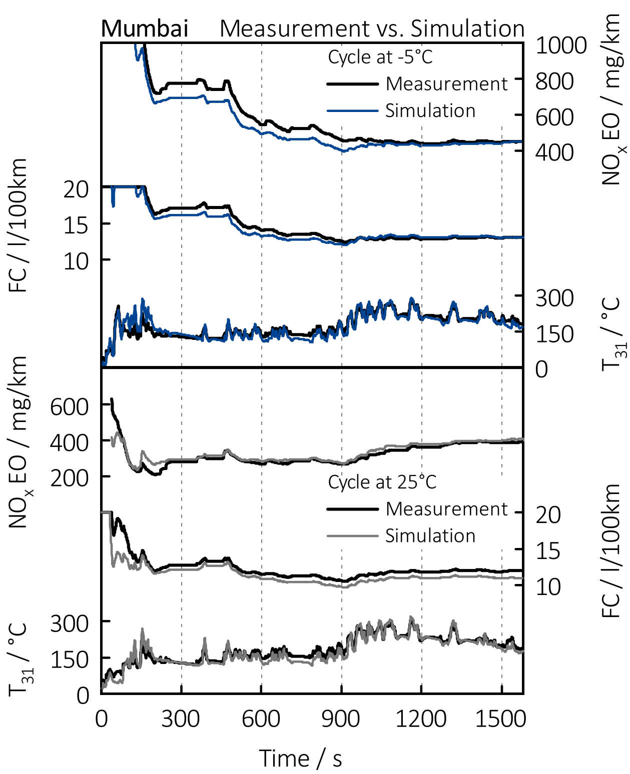


**Fig. 5** Comparison measurement vs. simulation in Mumbai city cycle at −5 °C and 25 °C ambient temperature

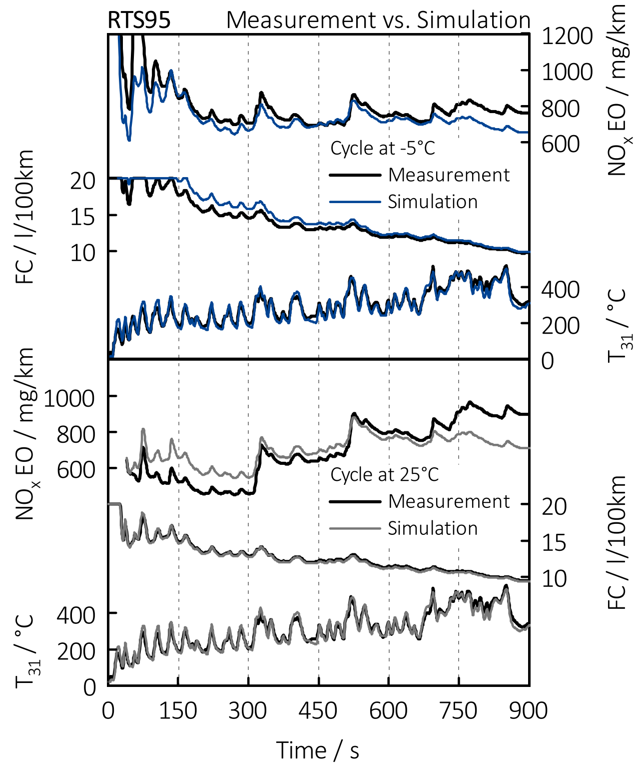


**Fig. 6** Comparison measurement vs. simulation in RTS95 at −5 °C and 25 °C ambient temperature

## 3 Results

The simulation environment is used to evaluate a possible technology package for EU 7. Specific emission boundaries are applied: (1) Those which are under discussion at Consortium for ultra-Low Vehicle Emissions (CLOVE) (considering only the higher limit "Scenario 1" [2]) and (2) an additional 8 km budget based on a proposal by ICCT [18], but in a modified form (i.e., with a higher 8 km budget of 240 instead of 200 mg $NO_x$, and a 30 instead of a 10 mg/km limit onwards). An overall consideration is that everything possible in the calibration is used to meet the defined emission limits. It is possible to limit the ICE and/or the powertrain performance within the first 2 km after the cold start in order to comply with the emission requirements. A detailed investigation with this torque or speed limitation was shown in [26]. With a proper hybridization, where the system power is comparable to a conventional powertrain, there is no impact to the drivability when the SOC stays in the target window. A detailed investigation about the extension of the altitude was not done until now. In addition to the driving cycles that were already used on the test bed, we consider new cycles that reflect borderline driving behavior expected to be included in the upcoming EU 7 legislation. Below, we describe the outcome of an analysis of the standard conditions, carried out to gather data on critical drive behaviors. In the following sections, a primary focus is placed on a 48 V P2 hybrid architecture.

An overview of the considered driving cycles is shown in Fig. 7. The cycles are listed according to their driving distance in km, starting from the top left and extending to the bottom right.

### 3.1 Baseline simulation

In the baseline simulation, we begin with the simulation matrix shown in Fig. 7. First, we evaluate the potential of the conventional powertrain, to meet the limitation without EHC and without the 48 V P2 module, plotted in Fig. 8. Second, we implement a 12 V EHC with a maximum heater power of 3 kW. Third, we configure the 48 V P2 module and a 48 V EHC with 4 kW maximum power. The HCU calibration is applied to all of the considered driving cycles. This ensures that the calibration can cover all possible application operating modes. The existing operation modes from the engine calibration are applied, and only the thresholds for activation and reactivation are adjusted for the vehicle scenario. The control of the energy management includes an active charge-sustaining mode from a 8 km driving distance and on to ensure that the required battery capacity is available to use all functionalities after restarting the engine (if required).

Because different driving cycles are considered, we partly need to perform a SoC correction of the fuel consumption for the 48 V MHEV configuration. The following correction formula 1 is applied, whereby the average brake-specific fuel consumption (BSFC), electrical efficiency and driving distance is used for the dedicated driving cycles. By making use of the average BSFC, the calculated result is not exact, but sufficiently accurate, since the SoC correction only affects a small fraction of the total consumption. A correction of pollutant emissions was not performed.

$$\Delta m_{\mathrm{Fuel}} = \frac{\Delta SoC_{48\mathrm{V}} \cdot BSFC_{\mathrm{Cycle\,avg}}}{\rho_{\mathrm{Fuel}} \cdot \eta_{\mathrm{el}} \cdot Distance} \tag{1}$$

Starting with the conventional powertrain without the EHC, the heating measure is limited to the ICE, as shown in Fig. 8. The results illustrated in the Fig. 9 indicate the potential of an 12 V EHC when operated with a 3 kW maximum power in the short and/or city cycles. In the short and low-load cycles, the emission results are improved but only at the cost of fuel consumption. The required energy for the EHC increases the cycle work per kilometer by around 10 % in the WLTC-3xLow and transport for London cycle (TFL), but

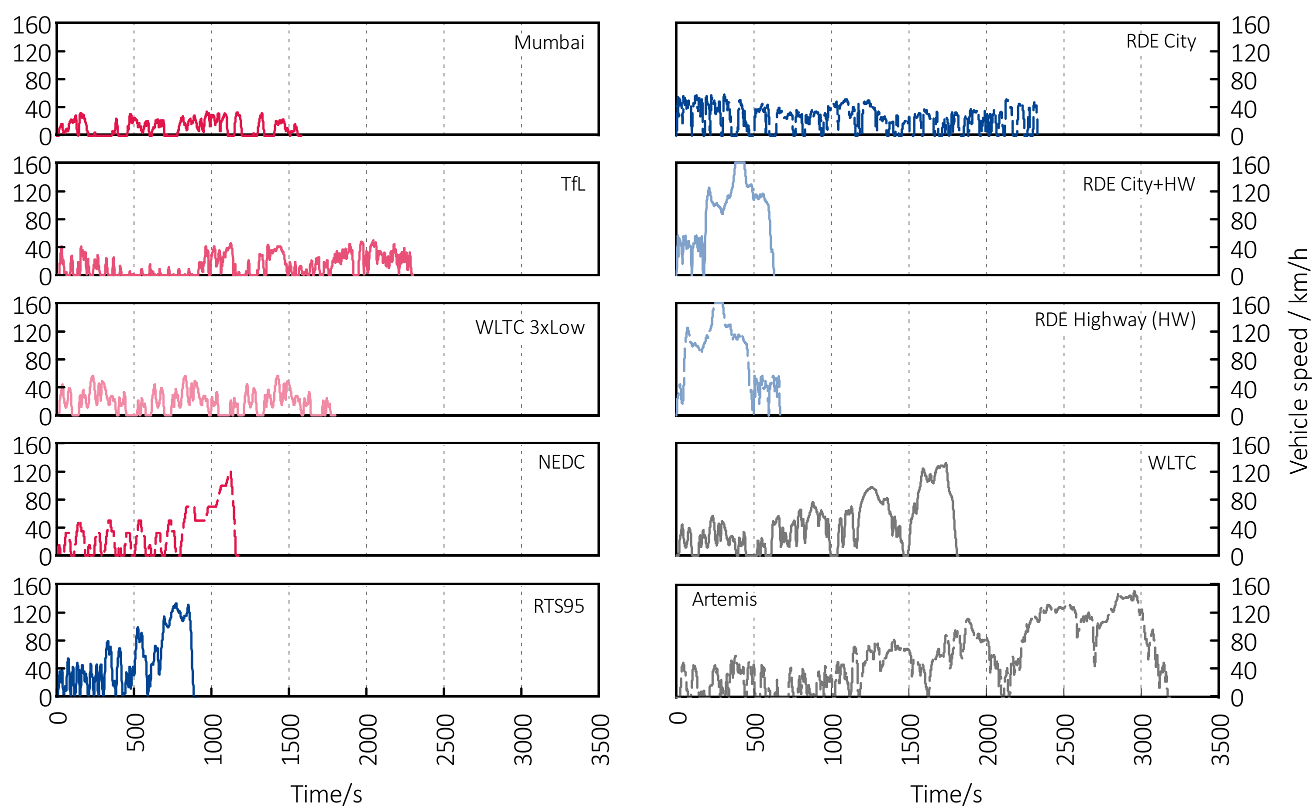


**Fig. 7** Cycle overview regarding vehicle velocity

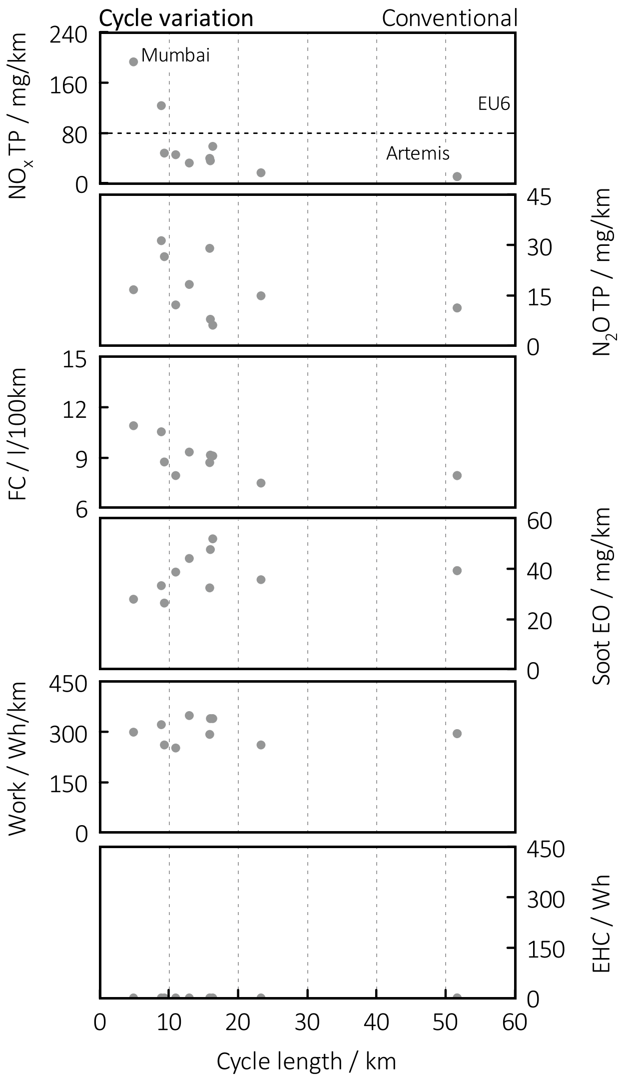


**Fig. 8** Conventional powertrain w/o EHC: Analysis of key parameters regarding the considered driving cycles

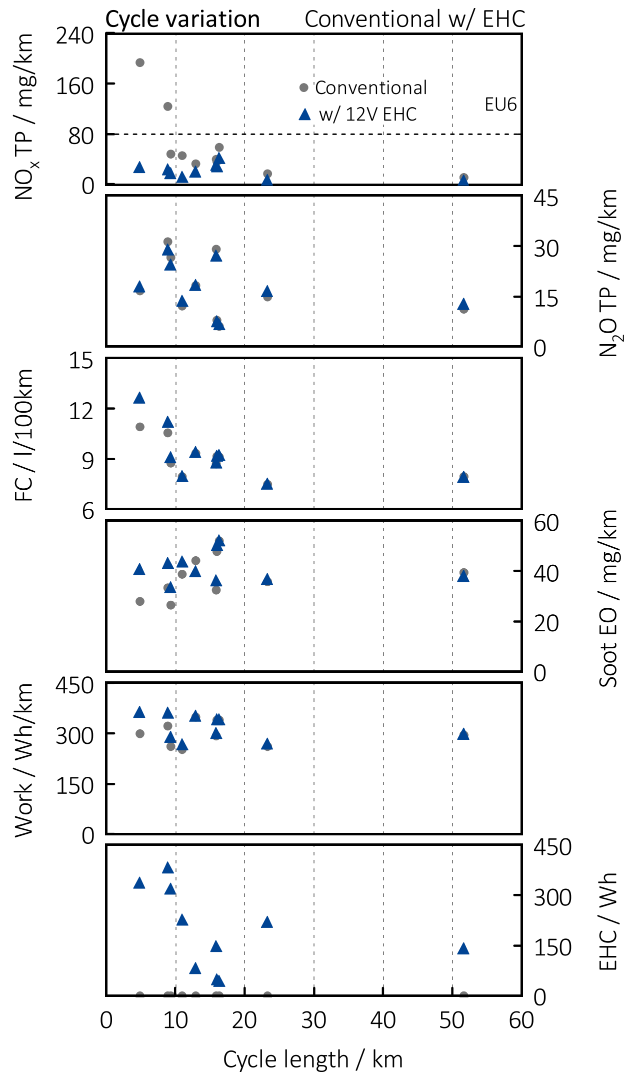


**Fig. 9** Conventional powertrain w/o and w/ EHC: Analysis of key parameters regarding the driving cycles considered

even by 20 % in the Mumbai City Cycle. In all other cycles with balanced driving settings, the impact is lower then 3 %, depending on the length of the cycles.

These results show that the new boundaries under discussion for the EU 7 legislation [2]—even for the moderate “Scenario 1” which is considered in this context—cannot be met with this propulsion and vehicle. Using the example of $NO_x$, “Scenario 1” means a limit value of 30 mg/km instead of 20 mg/km in “Scenario 2”. The potential of a conventional powertrain as considered previously is illustrated in Fig. 10. The area of the currently discussed power restriction up to 2 km is additionally marked [2]. Under standard conditions, the highway drive-up and the high dynamic city driving are the most critical drive behaviors regarding the $NO_x$ emissions. If we analyze the $N_2O$ emissions, however, the picture changes. The prevalence of certain side reactions, which result in the formation of $N_2O$ via SCR catalysts [13, 14], increases in cycles in which the greatest amount of $NO_x$ emissions are emitted at a defined temperature at the CC-SCR and/or the UF-SCR. $N_2O$ will still be considered as the most critical component, if it is still considered as a pollutant emission in the final EU 7 legislation. $N_2O$ emissions will always result from the use of copper SCR technologies, as a defined amount is formed via a side reaction during the main SCR reaction. Modern small-pore copper SCR catalysts generally release two $N_2O$ peaks—under low-temperature conditions from the decomposition of ammonium nitrate and under higher-temperature conditions due to $NH_3$ oxidation [14–16].

The emission tracks for carbon monoxide (CO), non-methane organic gases (NMOG) and methane ($CH_4$) are also shown in Fig. 11 for this conventional powertrain. CO does

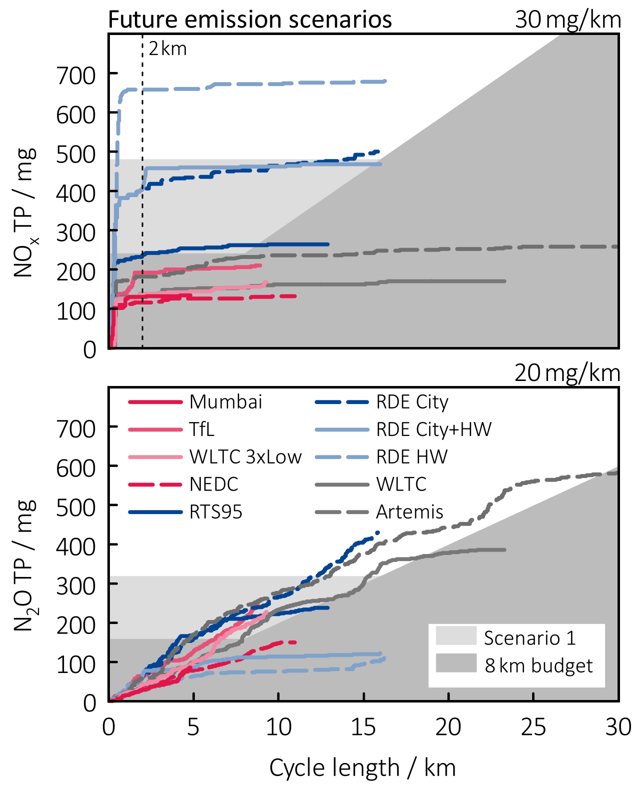


**Fig. 10** Conventional powertrain w/ EHC: $NO_x$ and $N_2O$ emissions versus EU 7 CLOVE proposal and 8 km budget

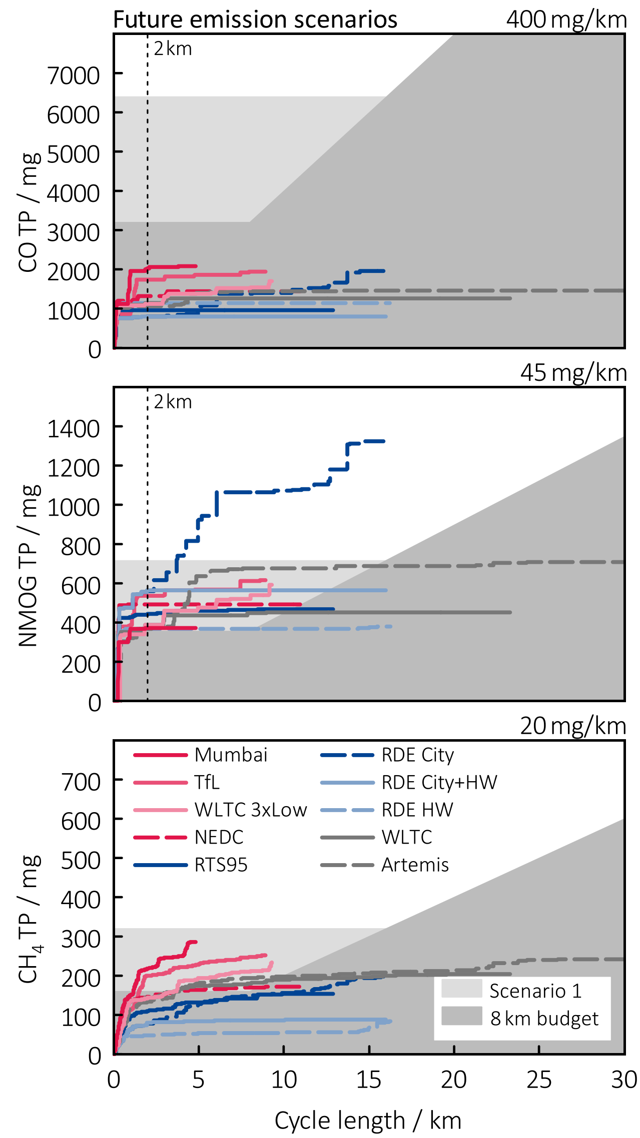


**Fig. 11** Conventional powertrain w/ EHC: NMOG/$CH_4$ and CO emissions versus EU 7 CLOVE proposal and 8 km budget

not pose a problem. Regarding NMOG and $CH_4$, almost all driving cycles fulfill the requirements described in the proposal of CLOVE—at least in the moderate "Scenario 1". Regarding the budget consideration of just 8 km, the results look different and, in fact, significantly worse.

For the ten driving cycles just shown, the shares of $N_2O$ and $NO_x$ tailpipe (TP) with respect to $NO_x$ EO emissions are clearly illustrated in Fig. 12. This figure shows that the ratio between $NO_x$ and $N_2O$ in terms of mass can sometimes vary significantly.

In the next step, the 48 V P2 configuration with 30 kW maximum power is taken into consideration. For the HCU, ICE and EAS calibration, the EASC is used to optimize the overall performance regarding the conversion of $NO_x$ and the emitted $CO_2$. The target for the $NO_x$ emission compliance is set to meet the specifications described in the CLOVE proposal, with the emission budget set at a 16 km driving distance. The main improvement seen when using the 48 V P2 configuration is the robustness of the $NO_x$-TP emissions and the $CO_2$ benefit, which are shown in Fig. 13.

The cumulative $NO_x$-TP cycle emissions are slightly lower than those seen with the conventional configuration and the 12 V EHC, among all of the considered driving cycles. This result is mainly due to the fact that the EM can reduce the EO-$NO_x$ and soot emissions by torque support near the full load. In addition, the $N_2O$ formed over the SCR catalysts is reduced, due to the lower $NO_x$ raw emission level. It would still be possible to use the 30 kW P2 EM and place a higher focus on the $NO_x$ emissions, but an increased $CO_2$ impact would result.

Plotting the derived results under standard conditions with consideration of the proposed EU 7 limits for $NO_x$ and $N_2O$, as shown in Fig. 14, we obtain a calibration and system layout that can be used to achieve the desired $NO_x$ for all cycles. The $N_2O$ emissions could be further reduced with support from the 48 V system, but the hardware and application currently limit any further reduction in the amounts of this species.

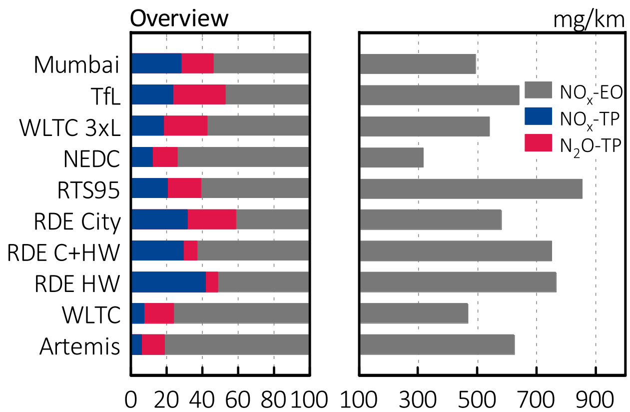


**Fig. 12** Conventional powertrain w/ EHC: share of $NO_x$ and $N_2O$ at TP measurement position

Finally, in Fig. 15, the $NO_x$-TP emissions of all three considered powertrain layouts are compared. Both the currently valid EU 6 limit value and the proposal for EU 7 are presented. Using a MHEV and the EHC, at least "Scenario 1" can be complied with in all cycles regarding these species.

## 3.2 Evaluation of lighter application

With the defined SUV application, it is possible to fulfill the $NO_x$ target. The $N_2O$ target is nearly achieved (i.e., on the borderline) as defined in the proposal from the CLOVE under standard ambient conditions. To determine the impact of carrying out a lighter application with the same hardware configuration, the same test cycles are investigated. In this context, "lighter" means less weight, less aerodynamic drag and less rolling resistance (cf. Table 3). The results of these investigations are plotted in Fig. 16. Based on the target calibration, the cycles identified as critical regarding $NO_x$-TP are similar to those identified in the previous evaluation. The $N_2O$ emissions improve, whereby the achieved tailpipe $N_2O$ remain below the proposed $N_2O$ target.

## 3.3 Ambient temperature impact in WLTC

Revisiting the defined heavy SUV application, it is possible to meet the $NO_x$ target and nearly to meet the $N_2O$ target (i.e., borderline results) as defined in the proposal. Next, we evaluate the impact of different ambient temperatures. The results of this evaluation are presented in Fig. 17. Based on the EASC and the hardware configuration, a stable $NO_x$ tailpipe emissions level can be maintained. The additional temperatures represent boundary conditions for the ambient temperature that are currently under discussion [2]. Based on the different ambient conditions and the correction of the engine calibration, the engine-out $NO_x$ emissions increase for −7 °C as well as for +35 °C. By increasing the $NO_x$-EO emissions, the $N_2O$ formation increases in parallel, leading to a violation of the proposed $N_2O$ emissions threshold.

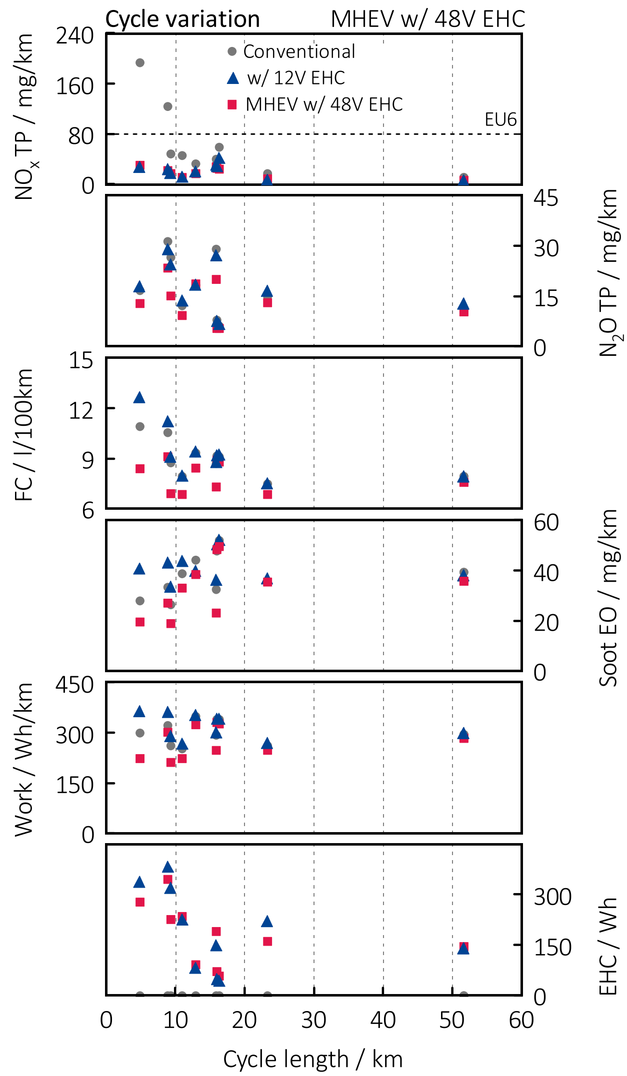


**Fig. 13** Conventional powertrain w/o and w/ EHC and MHEV w/ EHC: Analysis of key parameters regarding the driving cycles considered

## 3.4 P2 EM power impact

One important question must be answered to specify the hardware: Which MHEV system power and configuration is required? Therefore, it is important to consider the technical benefit against the system cost. We will evaluate different power ratings of the EM in the P2 configuration. First, we evaluate $NO_x$ and $N_2O$ on the basis of a WLTC, as shown in the Fig. 18. Regarding $NO_x$, all considered power ratings of the P2 EM yield similar $NO_x$ tailpipe emissions, but using a higher EM power rating reduces the $N_2O$ emissions.

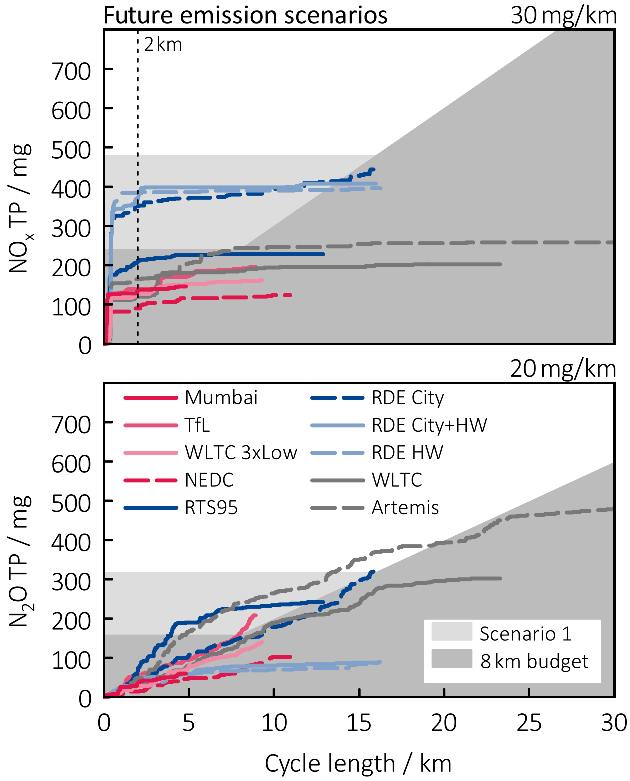


Fig. 14 MHEV powertrain w/ EHC: $NO_x$ and $N_2O$ emissions versus EU 7 CLOVE proposal and 8 km budget

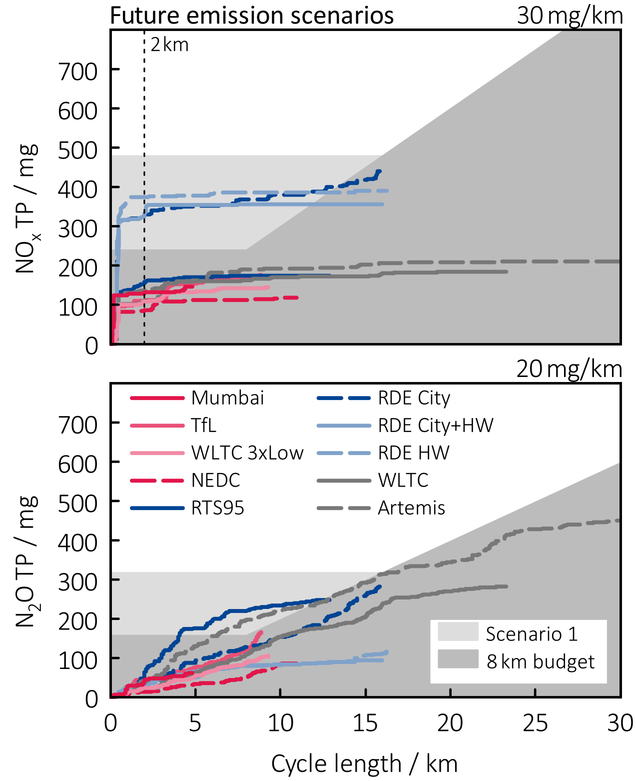


Fig. 16 MHEV powertrain for a lighter SUV: $NO_x$ and $N_2O$ emissions versus EU 7 CLOVE proposal and 8 km budget

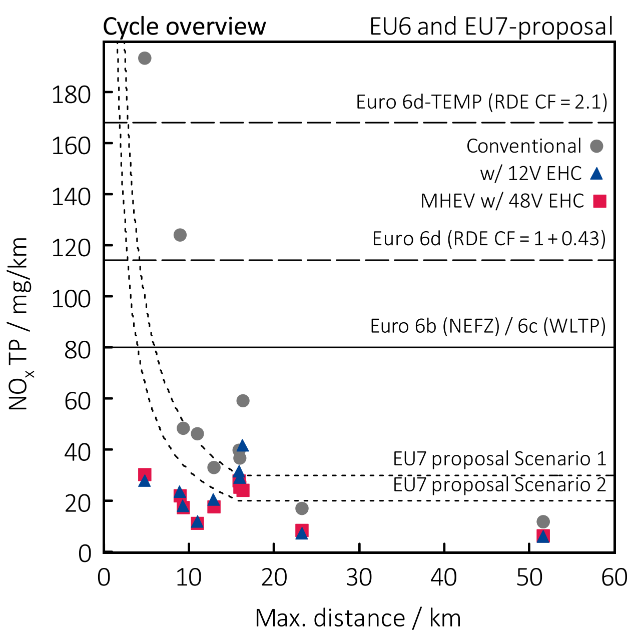


Fig. 15 Comparison of $NO_x$ cycle end emissions of conventional powertrain w/o and w/ EHC and MHEV w/ EHC

To properly evaluate the required P2 EM power rating, we need to consider a worst-case cycle with regard to the power demand. For this purpose, we evaluate a highway take-off cycle. The tailpipe $NO_x$ and $N_2O$ emissions are presented in Fig. 19. Compared to the WLTC, similar behavior for the divergent power ratings are observed. Regarding the emissions, it is not required to increase the power from 15 kW to 30 kW. The major advantage is the improvement in $CO_2$ emissions, as seen in all cycles that require more power. Thus, a balanced $CO_2$ benefit of 2 % can be achieved by increasing the power from 15 kW to 30 kW. Due to the huge $CO_2$ reduction potential, the comparison in Fig. 13 (MHEV w/ 48 V EHC) is presented at a peak power of 30 kW of the EM.

As a next step in the power rating evaluation, we focus on city driving; therefore, variations are performed in the TfL, and the results are shown in Fig. 20. Based on the calibration, the tailpipe $NO_x$ emissions for the different power ratings are comparable. Again, a $CO_2$ benefit between 15 kW and 30 kW is possible—in this case, even a benefit of 3 %.

Based on the $CO_2$ benefit by increasing the support potential of the MHEV system, a detailed analysis of the recuperation potential is conducted. Therefore, the braking energy provided by the EM is compared against the total available braking energy. Both the electrical braking and the efficiency achieved by reloading the battery are considered. Starting with the WLTC for the reference SUV application,

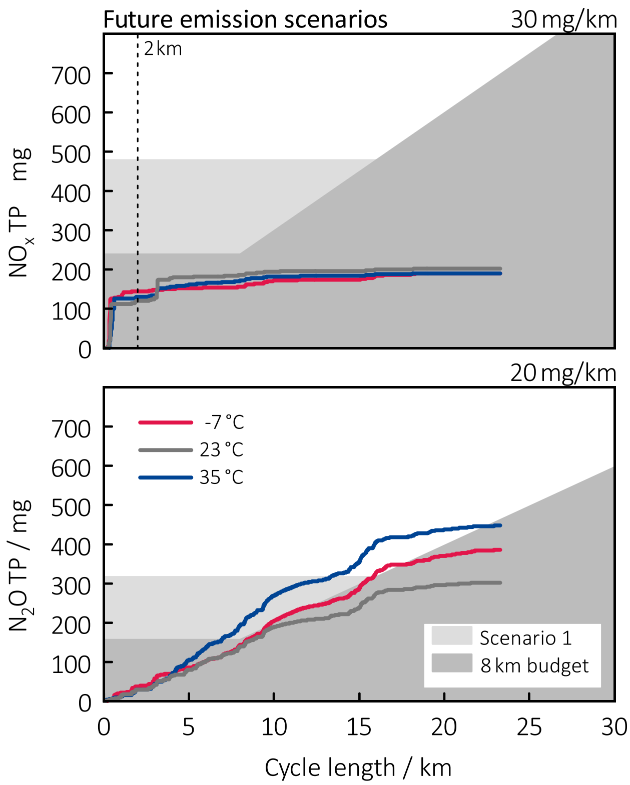


**Fig. 17** MHEV powertrain and WLTC: $NO_x$ and $N_2O$ emission evaluation at 23 °C, −7 °C and +35 °C

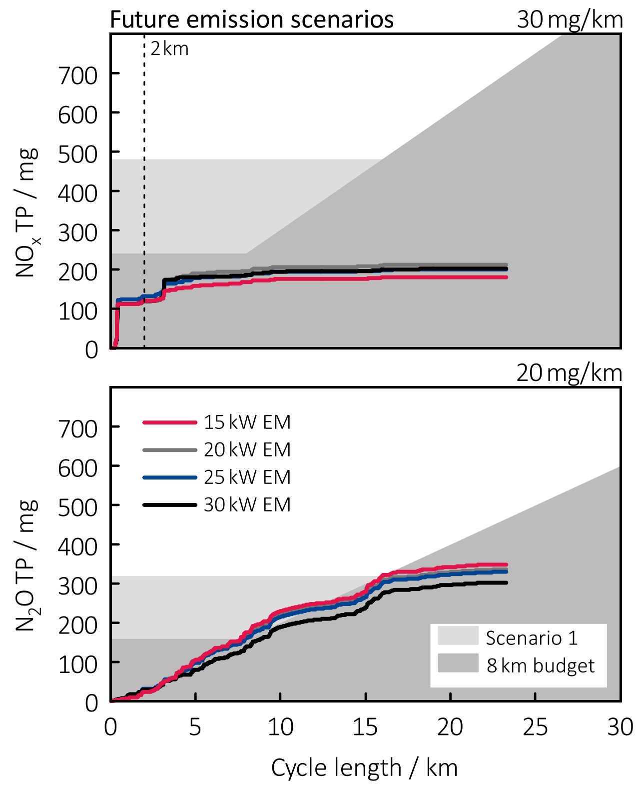


**Fig. 18** MHEV powertrain and WLTC: $NO_x$ and $N_2O$ emission evaluation at different P2 hybrid power levels (15 kW/20 kW/25 kW/30 kW) at 23 °C

the overall mechanical potential $\eta_{\text{Gross−EM}}$ (thus from the total available deceleration energy to the mechanical energy of the EM) with an 15 kW EM is around 70 % as shown in Fig. 21, meaning that only a small part of the overall braking energy needs to be provided by the mechanical brake. The driveability is also considered, which decreases the EM recuperation potential. By increasing the EM power to 30 kW, the EM braking potential can even be increased to 84 %. In the RTS95, the 15 kW application can cover only 58 % of the braking energy, due to the more dynamic behavior. In the 30 kW EM alternative application, the coverage can be increased to 76 %. Considering the lower dynamic range, as in the TfL, the lower power rating can cover 72 % at 15 kW and 85 % at 30 kW.

A comparison of the full-load operation ratio of the EM $\eta_{\text{FL−ratio EM}}$ provides an indication of the load during recuperation as compared to its maximum power during recuperation, thus durability. While the 15 kW EM operates on between 60 % and 80 % of the rated power on average, the 30 kW EM reduces the share to between 50 % and 60 %.

The last bars represent the average efficiency of the EM $\eta_{\text{EM}}$—thus, the electrical divided by the mechanical energy. Multiplying $\eta_{\text{Gross−EM}}$ by $\eta_{\text{EM}}$ gives the total recuperation efficiency from gross energy to electrical energy of the EM.

### 3.5 Hybrid mode share analysis

For a specific driving cycle, there will be always a different share of active MHEV operation modes. In particular, this is affected because of the constraint that a forced charge sustaining is triggered to prepare the MHEV system for a possible restart at a distance of 8 km. Next, a separate mode share analysis is performed for defined distances to see how long (i.e., in terms of distance) each hybrid mode is activated.

The results of the analysis of the mode share in the WLTC within the first 2 km indicate that there is a clear focus on torque support for the EAS intervention. For around 27 % percent of this distance, the EAS coordinator requests specific torque support to enable optimal operation conditions for the aftertreatment, as shown in Fig. 22. To heat up the EAS as soon as possible, the electrical driving mode is not beneficial. This is also evident within the first 2 km, whereby only 4 % of the distance are operated in a purely electrical mode. Within the first 8 km, the share changes. At around 15 % of this operation distance, the EV mode is used to optimize the $CO_2$ in this operation area. The EAS intervention is also reduced, because the EAS light-off of the CC-SCR can be achieved.

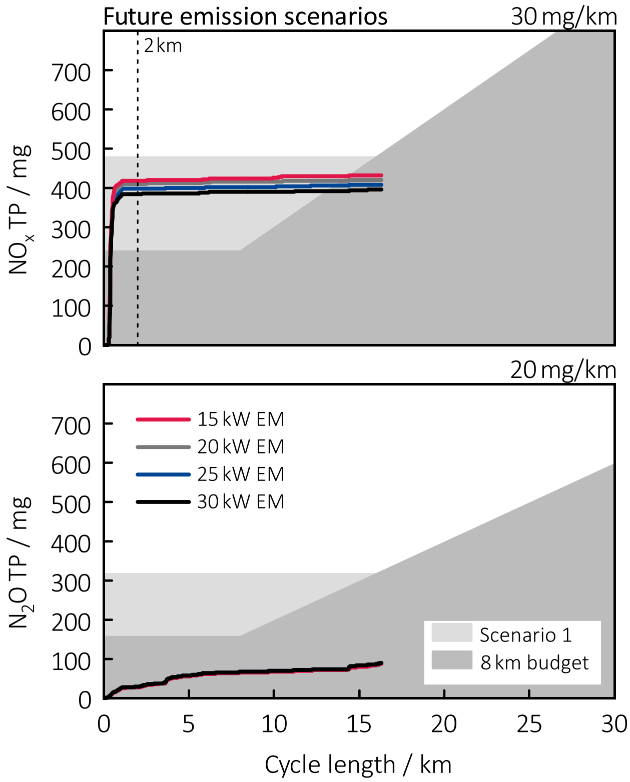


**Fig. 19** MHEV powertrain and RDE-HW: $NO_x$ and $N_2O$ emission evaluation at different P2 hybrid power levels (15 kW/20 kW/25 kW/30 kW) at 23 °C

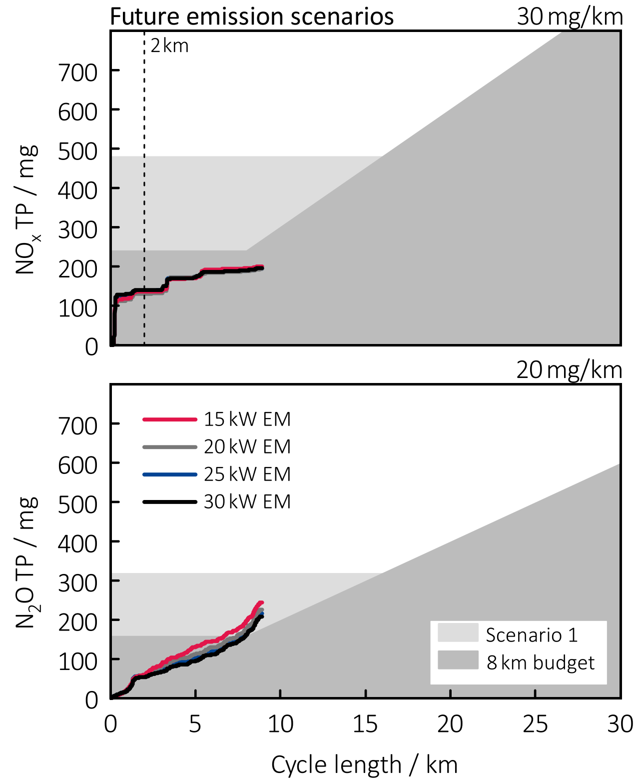


**Fig. 20** MHEV powertrain and TfL: $NO_x$ and $N_2O$ emission evaluation at different P2 hybrid power levels (15 kW/20 kW/25 kW/30 kW) at 23 °C

The TfL is then considered to evaluate the mode share from the HCU, as shown in Fig. 23. Due to the low speed and the high idle ratio of the test cycle, the heat-up and support for the ICE are considered as key elements for the $NO_x$ emission optimization and $CO_2$ reduction. Around 17 min are needed to reach the 2 km threshold in the TfL. As compared to the WLTC, the 2 km threshold is reached within the first 5 min. Using combined heating, considering ICE, EHC and the support of a proper EAS intervention, and thus avoiding inefficient low-load operation points, the light-off can be reached within the first 2 km. The share of the EAS intervention is 18.5 % and the EV operation is 19 % at this distance. This means that the $CO_2$ emissions are actively optimized using the MHEV system within the first 2 km. Based on the SoC recovery calibration, the MHEV system is used to restore the initial energy level of the 48 V battery. Within 8 km and near the end of the cycle (i.e., 8.9 km), the focus is mainly on the LPU, which covers 37 % of the total operation distance. In the complete TfL, 16 % of the distance can be covered without the support of the MHEV (i.e., pure ICE driving).

The RTS95 cycle shows a high dynamic and a generally high-load request. The first 2 km are reached in just over 5 min, whereby the vehicle operation is characterized by several accelerations of up to 50 km/h, including subsequent decelerations to come to a stop. This behavior is evaluated with a ratio of 40.6 % in the recuperation mode (depicted in Fig. 24) and of only 9 % in the EAS intervention mode, which mainly takes into account the ICE load reduction. Throughout the RTS95, the conventional operation with the ICE provides 24 % of the distance. This result shows that the ICE still represents an efficient and reasonable power source. As in the WLTC and the TfL, the LPU is also applied in the RTS95 and specifically at 34.2 % to balance the battery energy and ensure a fair $CO_2$ evaluation.

## 4 Summary and outlook

To protect the environment and especially the human health, we must minimize the emissions. We cannot neglect the negative influences of all that has happened up until now, but we must minimize the consequences in the future. To ensure public transport and the transport of goods, we need to find a compromise between what is technically possible and what is a technically reasonable solution regarding the planned EU 7 emission regulation. Therefore, the

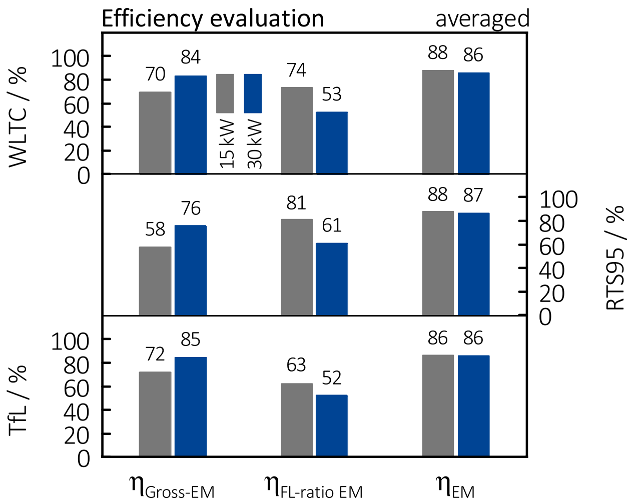


**Fig. 21** Recuperation potential at WLTC, RTS95 and TfL

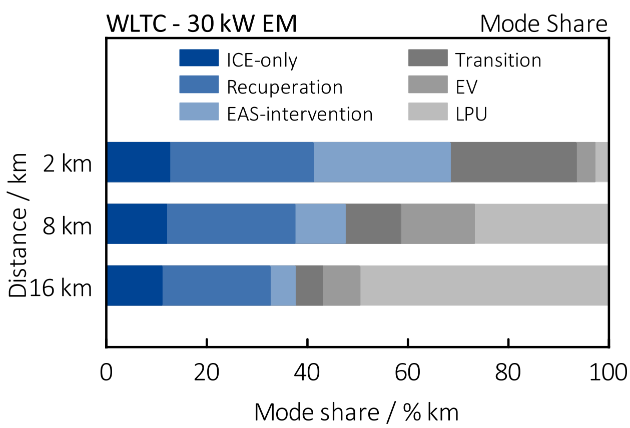


**Fig. 22** Hybrid mode share in WLTC at 30 kW EM power for 2 km, 8 km and 16 km

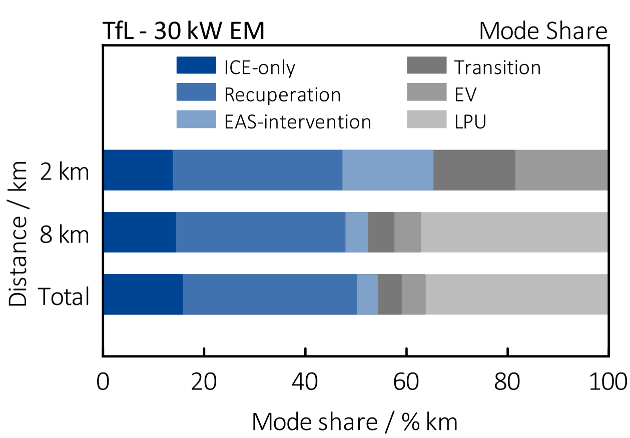


**Fig. 23** Hybrid mode share in the TfL at 30 kW EM-power for 2 km, 8 km and Total (8.9 km)

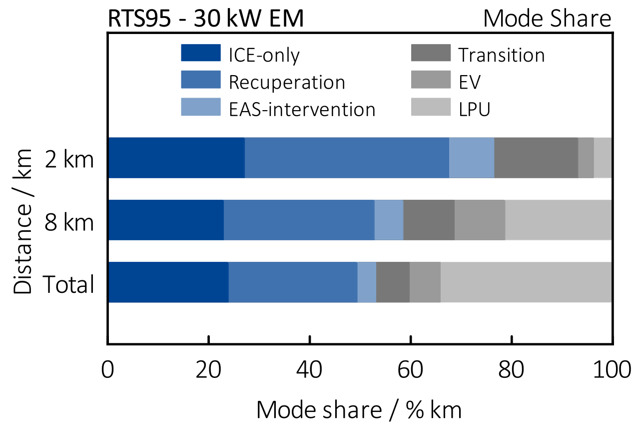


**Fig. 24** Hybrid mode share in the RTS95 at 30 kW EM power for 2 km, 8 km and Total (12.9 km)

investigated diesel-ICE-based powertrains can be considered as emission compliant, considering the currently proposed boundaries and emission limits. Regarding the simulation outputs for the heavy and lighter SUV, $N_2O$ is a borderline pollutant, the emission of which is directly linked to the EAS configuration, $NO_x$-EO emissions and the applied aftertreatment technology.

The EAS configuration was selected to avoid a lean $NO_x$ trap (LNT), due to the impact of the $N_2O$ and $CH_4$ emissions during a requested active purge event [13]. Regarding the engine-out emissions, $N_2O$ forms in the DOC light-off area [13, 17], especially during the heat-up period, which is affected by the total hydrocarbons (THC) and CO. After reaching the DOC light-off, the engine-out $NO_x$ emissions are limited on the lower side by the maximum tolerable soot level and the component limits of the selected engine hardware. The main $N_2O$ production source is the SCR system, in this case copper SCR zeolites, that are state of the art for PC and LCV applications. The coating companies need to optimize the trade-off between $NO_x$ conversion and $N_2O$ formation as a side reaction. No comparable SCR coating is available that offers similar $NO_x$ conversion rates and the same long-term temperature stability.

Within the simulation activities some possible powertrain configurations for a given engine and EAS hardware are evaluated. The boundaries are linked to the proposed EU 7 content from the CLOVE and the ICCT. This will probably change when the final legislation text is published by the European Commission. In the created simulation environment, the effort required to change the calibration based on adapted emission targets is manageable within a limited amount of time. Changing the aftertreatment technology or even the arrangement is also feasible within a short time frame. By challenging the system to optimize the controller or hardware settings for dedicated scenarios, using design of experiments (DoE) with AVL CAMEO™ is both possible and reasonable [4]. Based on these benefits, this system model operated with the simulation platform AVL CRUISE™ M Model.CONNECT™ is appropriate for carrying out specific tasks early on in the pre-development phase.

Beside the considered boundaries, which are covering critical conditions within the EU7 proposal from the CLOVE and the ICCT, there are other possible cycles and driving boundaries. In addition to the $NO_x$ and $N_2O$ emissions, other pollutants can be critical depending on the EAS layout, target application and the used calibration. What will also be challenging are the particulate numbers for 23 nm and 10 nm, but for this, the current used simulation platform is not yet suitable to predict. For this evaluation, there were no product tolerances or additional aging phenomena considered, which is important to show the robustness of the application and the possibilities for OBD/OBM. To find an indication on the emission impact and difficulty, please refer to [27].

## Appendix

See Tables 1, 2, 3.

**Acknowledgements** These investigations were carried out as part of the COMET research project "RC-LowCAP", which is funded by the Austrian Research Promotion Agency (FFG) and the industry partners mentioned below. The cooperation of and provision of individual exhaust components by members of the research consortium, consisting of AVL, Vitesco Technologies Emitec and Heraeus, made this study possible.

**Table 1** ICE and EM characteristics, emission measures

| | |
|---|---|
| Cylinder | Straight-four |
| Ignition | Compression ignition |
| Fuel | Diesel oil |
| Displacement | 2000 $cm^3$ |
| Compression ratio | 16.5 |
| Injection system | Common-rail |
| Injection pressure | 2000 bar |
| Turbocharger | Single stage |
| Number of valves | 4 |
| Max. cylinder pressure | 150 bar |
| Rated speed | 4400 $min^{-1}$ |
| $V_{EM}$ | 48 V |
| $P_{EM\,max}$ | 30 kW |
| $n_{EM\,max}$ | 18,000 $min^{-1}$ |
| $M_{EM\,max}$ | 57 Nm |
| $i_{EM}$ | 3.5 |
| $C_{BAT}$ | 2.3 kWh |
| Emission measures | Cooled HP-EGR (bypass) |
| | 48V EHC (4kW peak power) |
| | Diesel oxidation catalyst (DOC) |
| | Diesel particulate filter (DPF) |
| | Double-dosing SCR system |

**Table 2** Exhaust gas aftertreatment system

| Catalyst | Volume | Ø | Coating | CPSI | Information |
|---|---|---|---|---|---|
| EHC | 0.1 l | 5.66" | – | 130 | – |
| DOC | 1.95 l | 5.66" | 140 g/$ft^3$ | 600 | Pt:Pd=4:1 |
| SCR | 2 l | 7" | 200 g/l | 400 | EU6d final |
| sDPF | 3 l | 7" | 95 g/l | 300 | EU6d final |
| UF-SCR | 4.8 l | oval | – | – | incl. ASC |

**Table 3** Vehicle driving resistance parameters

| Parameter | Standard SUV | Light SUV |
|---|---|---|
| Test mass high / kg | 2264 | 2000 |
| R0 / N | 240 | 144.7 |
| R1 / N/(km/h) | 0.37 | 0.903 |
| R2 / N/$(km/h)^2$ | 0.0471 | 0.0334 |

**Funding** Open access funding provided by Graz University of Technology.

## Declarations

**Conflict of interest** The authors declare that they have no conflict of interest.



## References

1. Council Directive 91/441/EEC: Official Journal. L 242. (1991)
2. CLOVE Consortium: Additional technical issues for Euro 7 LDV. 10th AGVES-Meeting on 27th April 2021. (2021). https://circabc.europa.eu/sd/a/451ffbfb-b095-41bc-a4df-1a15af9f1409/AGVES-2021-04-27-LDV_v7_final.pdf. Accessed February 10th, (2022)
3. Kühberger, G., Wancura, H., Nenning, L., Schutting, E.: Current experimental developments in 48 V-based CI-driven SUVs in response to expected future EU7 legislation. Automot. Engine Technol. (2021). https://doi.org/10.1007/s41104-021-00095-0

4. Kreis, C., Scheidel, S.: ICE - The Path to Zero Impact Emission: DOE based Hybrid Strategy Optimization. AVL Virtual International Simulation Conference 2021. (2021)
5. Martin, C., Weißbäck, M., Goetschl, P., Wancura, H., Kapus, P., Fraidl, G., Krapf, S., Seewald, G., Steinhaus, T., Thiem, M., Beidl, C.: Zero Impact Emission vs. Affordability – The ICE as Part of the Solution. 29th Aachen Colloquium Sustainable Mobility 2020. Aachen. (2020)
6. Borgeest, K.: Manipulation von Abgaswerten: Technische, gesundheitliche, rechtliche und politische Hintergründe des Abgasskandal. 2nd Edition. SpringerVieweg Wiesbaden. (2021). https://doi.org/10.1007/978-3-658-32811-5
7. Fuckar, G., Böhm, H., Schöffmann, W., Hoffmann, S.: 48-V-P2-Modul für Quermotoren - Von der Auslegung zur Umsetzung. MTZ Motortech Z. Issue 80. Page 62–67. (2019). https://doi.org/10.1007/s35146-019-0096-0
8. Mitterecker, H., Wancura, H., Weißbäck, M., Hoffmann, S.: Der elektrifizierte Diesel - Vom Konzept zur Fahrzeugintegration. MTZ Motortech Z. Issue 80. Page 18–27. (2019). https://doi.org/10.1007/s35146-019-0119-x
9. Wancura, H., Weißbäck, M., Hoffmann, S., Unterberger, B.: Der elektrifizierte Diesel als nachhaltige Zukunftslösung. MTZ Motortech Z. Issue 81. Page 30-35. (2020). https://doi.org/10.1007/s35146-020-0326-5
10. Commission Regulation (EU) 2016/427: Official Journal of the European Union. L 82. (2016)
11. Commission Regulation (EU) 2018/1832: Official Journal of the European Union. L 301. (2018)
12. Schoeffmann, W., Howlett, M., Enzi, B., Sams, C., Weißbäck, M.: Future Diesel-Powertrain in LCV and SUV-Electrified, Modular Platform with Focus on Emission, Efficiency and Cost. SAE Technical Paper Series. (2021). https://doi.org/10.4271/2021-01-0635
13. Hausberger, S., Kufferath, A.: EURO 7: The coming regulation between challenge and feasibility. 18th Symposium Sustainable Mobility, Transport and Power Generation. Graz. (2021)
14. Xi, Y., Ottinger, N. A., Keturakis, C. J., Liu, Z. G.: Dynamics of low temperature $N_2O$ formation under SCR reaction conditions over a Cu-SSZ-13 catalyst. Applied Catalysis B: Environmental. 294. 120245. (2021). https://doi.org/10.1016/j.apcatb.2021.120245
15. Li, S., Zhang, C., Zhou, A., Li, Y., Yin, P., Mu, C., Xu, J.: Experimental and kinetic modeling study for $N_2O$ formation of $NH_3$ -SCR over commercial Cu-zeolite catalyst. Advances in Mechanical Engineering. 13(4). 168781402110106. (2021). https://doi.org/10.1177/16878140211010648
16. Liu, B., Yao, D., Wu, F., Wei, L., Li, X., Wang, X.: Experimental investigation on $N_2O$ formation during the selective catalytic reduction of $NO_x$ with $NH_3$ over Cu-SSZ-13. Ind. Eng. Chem. Res. **58**(45), 20516–20527 (2019). https://doi.org/10.1021/acs.iecr.9b03294
17. Kamasamudram, K., Henry, C., Currier, N., Yezerets, A.: $N_2O$ formation and mitigation in diesel aftertreatment systems. SAE Int. J. Eng. 5 (2012). https://doi.org/10.4271/2012-01-1085
18. ICCT: ICCT's comments and technical recommendations on future Euro 7/VII emission standard. https://theicct.org/comments-to-the-european-commission-on-the-development-of-euro-7-vii-pollutant-emission-standards-for-cars-trucks-and-buses/. Accessed February 10th (2022)
19. Eichlseder, H., Hausberger, S., Beidl, C., Steinhaus, T.: Zero impact—objective and significance for vehicle powertrains and air quality. 8th International Engine Congress Baden-Baden (2021)
20. Hausberger, S., Uhrner, U., Stadlhofer, W., Toenges-Schuller, C., Schnieder, C.: Zero-Impact-Fahrzeuge. 31st Aachen Colloquium Sustainable Mobility (2022)
21. Glatz, T., Kutschi, S., Wurzenberger, J.C.: Virtual Test Bed - What does this mean for Aftertreatment Modeling. Bad Herrenalb/Karlsruhe, International Symposium on Modeling of Exhaust-Gas After-Treatment (MODEGAT VII), KIT (2022)
22. Knaus, O., Wurzenberger, J. C.: System Simulation in Automotive Industry. In: Hick, H., Küpper, K., Sorger, H. (Eds.): Systems Engineering for Automotive Powertrain Development, Springer. https://doi.org/10.1007/978-3-319-99629-5
23. Wurzenberger, J. C., Heinzle, R., Deregnaucourt, M.-V., Katrasnik, T.: Comprehensive Study on Different System Level Engine Simulation Models. SAE Technical Paper 2013-01-1116, SAE International (2013)
24. Danninger, A., Mustedanagic, I., Herbst, M., Kreuzberger, C., Lichtenberger, P.L., Wabnig, A., Zehetner, J., Macher, G., Armengaud, E.: Smart environment for the efficient validation of innovative exhaust after-treatment systems on multicore engine control (2017)
25. Glensvig, M., Kozlik, C., Kreilinger, D.: Full vehicle virtual calibration platform. 20. VDI-Kongress mit Fachausstellung SIMVEC (2022)
26. Wancura, H., Kreis, Chr., Krapf, S.: Euro 7/VII – Prospects of the Diesel Engine for the LCV Segment. 12th Int. AVL Emissions and Energy Forum (2022)
27. Gunja, R., Wancura, H., Raser, B., et al.: Euro 7/VII concepts in the interaction with OBD/OBM. MTZ Worldw **83**, 44–51 (2022). https://doi.org/10.1007/s38313-022-0852-2